AMERICAN SOCIETY FOR MICROBIOLOGY | mSphere®

RESEARCH ARTICLE

Pyoverdine Inhibitors and Gallium Nitrate Synergistically Affect *Pseudomonas aeruginosa*

Donghoon Kang,[a] Alexey V. Revtovich,[a] Alexander E. Deyanov,[a] Natalia V. Kirienko[a]

[a]Department of BioSciences, Rice University, Houston, Texas, USA

ABSTRACT *Pseudomonas aeruginosa* is a multidrug-resistant, opportunistic pathogen that frequently causes ventilator-associated pneumonia in intensive care units and chronic lung infections in cystic fibrosis patients. The rising prevalence of drug-resistant bacteria demands the exploration of new therapeutic avenues for treating *P. aeruginosa* infections. Perhaps the most thoroughly explored alternative is to use novel treatments to target pathogen virulence factors, like biofilm or toxin production. Gallium(III) nitrate is one such agent. It has been recognized for its ability to inhibit pathogen growth and biofilm formation in *P. aeruginosa* by disrupting bacterial iron homeostasis. However, irreversible sequestration by pyoverdine substantially limits its effectiveness. In this report, we show that disrupting pyoverdine production (genetically or chemically) potentiates the efficacy of gallium nitrate. Interestingly, we report that the pyoverdine inhibitor 5-fluorocytosine primarily functions as an antivirulent, even when it indirectly affects bacterial growth in the presence of gallium, and that low selective pressure for resistance occurs. We also demonstrate that the antibiotic tetracycline inhibits pyoverdine at concentrations below those required to prevent bacterial growth, and this activity allows it to synergize with gallium to inhibit bacterial growth and rescue *Caenorhabditis elegans* during *P. aeruginosa* pathogenesis.

IMPORTANCE *P. aeruginosa* is one of the most common causative agents for ventilator-associated pneumonia and nosocomial bacteremia and is a leading cause of death in patients with cystic fibrosis. Pandrug-resistant strains of *P. aeruginosa* are increasingly identified in clinical samples and show resistance to virtually all major classes of antibiotics, including aminoglycosides, cephalosporins, and carbapenems. Gallium(III) nitrate has received considerable attention as an antipseudomonal agent that inhibits *P. aeruginosa* growth and biofilm formation by disrupting bacterial iron homeostasis. This report demonstrates that biosynthetic inhibitors of pyoverdine, such as 5-fluorocytosine and tetracycline, synergize with gallium nitrate to inhibit *P. aeruginosa* growth and biofilm formation, rescuing *C. elegans* hosts during pathogenesis.

KEYWORDS *Caenorhabditis elegans*, *Pseudomonas aeruginosa*, fluorocytosine, gallium, pyoverdine, tetracycline

Pseudomonas aeruginosa is a Gram-negative, multidrug-resistant, opportunistic pathogen that threatens the lives of hospitalized patients, especially those in intensive care units. *P. aeruginosa* is one of the most common causes of ventilator-associated pneumonia (VAP) in these environments and has a high attributable mortality rate (1, 2). The importance of treating nosocomial VAP has become critical amid the coronavirus disease 2019 (COVID-19) pandemic, particularly since early studies have identified *P. aeruginosa* as one of the most common bacterial pathogens in COVID-19 patients (3, 4). *P. aeruginosa* also frequently infects patients who are immunocompromised due to cancer (5) and is the leading cause of chronic lung infections in patients with cystic fibrosis (6). Unfortunately, it is becoming increasingly difficult to treat *P. aeruginosa* infections due to the rising prevalence of drug-resistant strains. For example,

Citation Kang D, Revtovich AV, Deyanov AE, Kirienko NV. 2021. Pyoverdine inhibitors and gallium nitrate synergistically affect *Pseudomonas aeruginosa*. mSphere 6:e00401-21. https://doi.org/10.1128/mSphere.00401-21.

Editor Patricia A. Bradford, Antimicrobial Development Specialists, LLC

Address correspondence to Natalia V. Kirienko, kirienko@rice.edu.

Received 29 April 2021
Accepted 26 May 2021
Published 16 June 2021

our recent survey of multidrug-resistant *P. aeruginosa* isolates from pediatric patients with cystic fibrosis determined that a substantial fraction of the isolates were resistant to aminoglycosides, third- and fourth-generation cephalosporins, and even carbapenems, which are considered antibiotics of last resort for treating *P. aeruginosa* (7). The combination of increasing antibiotic resistance and the dwindling rate of new drug development is creating an urgent need for new therapeutics to treat these infections.

Recent work has bolstered the concept of targeting virulence determinants as an alternative treatment route. One common target is the siderophore pyoverdine, which is essential for bacterial growth under iron-restricted conditions, including during mammalian infections (8–11). Pyoverdine also regulates the production of secreted toxins such as the translational inhibitor exotoxin A and the protease PrpL (12). Interestingly, pyoverdine also disrupts host iron and mitochondrial homeostasis, even in the absence of the pathogen (13–16). A combination of these factors makes pyoverdine obligatory for *P. aeruginosa* virulence in murine lung infection models (9, 11, 17). Treatments that block pyoverdine biosynthesis (like the fluoropyrimidines 5-fluorocytosine or 5-fluorouridine) or pyoverdine function (like the small molecules LK11 or PQ3c) can substantially improve host survival under these conditions (7, 18–21).

Gallium(III) nitrate, $Ga(NO_3)_3$, has received considerable attention as an antipseudomonal therapeutic and has been shown to mitigate *P. aeruginosa* virulence in several murine infection models (22, 23). The widespread use of iron for redox biology across many metabolic pathways makes $Ga(NO_3)_3$ an effective antimicrobial (24). The most common explanation is that gallium(III) competes for binding sites in bacterial proteins and other molecules that are normally occupied by redox-active iron(III) (25). Since gallium(III) has an almost identical ionic radius but is redox inactive, its occupancy of these sites dramatically compromises their function.

In this report, we recapitulate previous findings that pyoverdine provides resistance to $Ga(NO_3)_3$ and extend them by showing that preventing pyoverdine biosynthesis potentiates gallium's antimicrobial activity. We show that the pyoverdine inhibitor 5-fluorocytosine synergizes with $Ga(NO_3)_3$ to inhibit *P. aeruginosa* growth and rescue *Caenorhabditis elegans*. We also demonstrate that this antivirulent maintains its low selective pressure for resistance even when it indirectly contributes to the inhibition of *P. aeruginosa* growth. Finally, we report that tetracycline-class antimicrobials attenuate pyoverdine production at concentrations lower than those that prevent bacterial growth, exhibiting synergistic interactions with gallium nitrate *in vitro* and *in vivo*.

RESULTS

Pyoverdine production confers gallium(III) nitrate resistance to *P. aeruginosa*. By virtue of being a ferric iron mimetic, gallium(III) is subject to chelation by the *P. aeruginosa* siderophores pyochelin and pyoverdine. Interestingly, this appears to have divergent effects depending upon which siderophore binds the metal. When pyochelin binds gallium(III), it deposits the metal into the cell where it interferes with cell function. Consequently, a pyochelin biosynthetic mutant, like *P. aeruginosa* Δ*pchBA* is more resistant to $Ga(NO_3)_3$ than wild-type *P. aeruginosa* (see Fig. S1 in the supplemental material). In contrast, pyoverdine appears to sequester gallium either outside the bacterium or within the periplasmic space (24, 26, 27), and *P. aeruginosa* Δ*pvdF*, which has compromised pyoverdine biosynthesis, is more susceptible to $Ga(NO_3)_3$ than wild-type *P. aeruginosa* in iron-limited media (Fig. 1A and B). This effect is abolished under conditions where pyoverdine is superfluous for survival, such as iron-rich media (Fig. 1C and D).

5-Fluorocytosine synergizes with gallium nitrate to inhibit *P. aeruginosa* growth and virulence. Since pyoverdine production confers resistance to $Ga(NO_3)_3$, we predicted that compounds that prevent pyoverdine biosynthesis would potentiate the antimicrobial activity of gallium(III). Recent work has demonstrated that fluoropyrimidines (including 5-fluorocytosine, 5-fluorouridine, and 5-fluorouracil) inhibit pyoverdine production (18, 21). In particular, 5-fluorocytosine (5-FC) has been repeatedly shown to attenuate *P. aeruginosa* virulence during murine lung infection without exhibiting overt antibacterial activity *in vitro* (7, 18). We tested the interactions

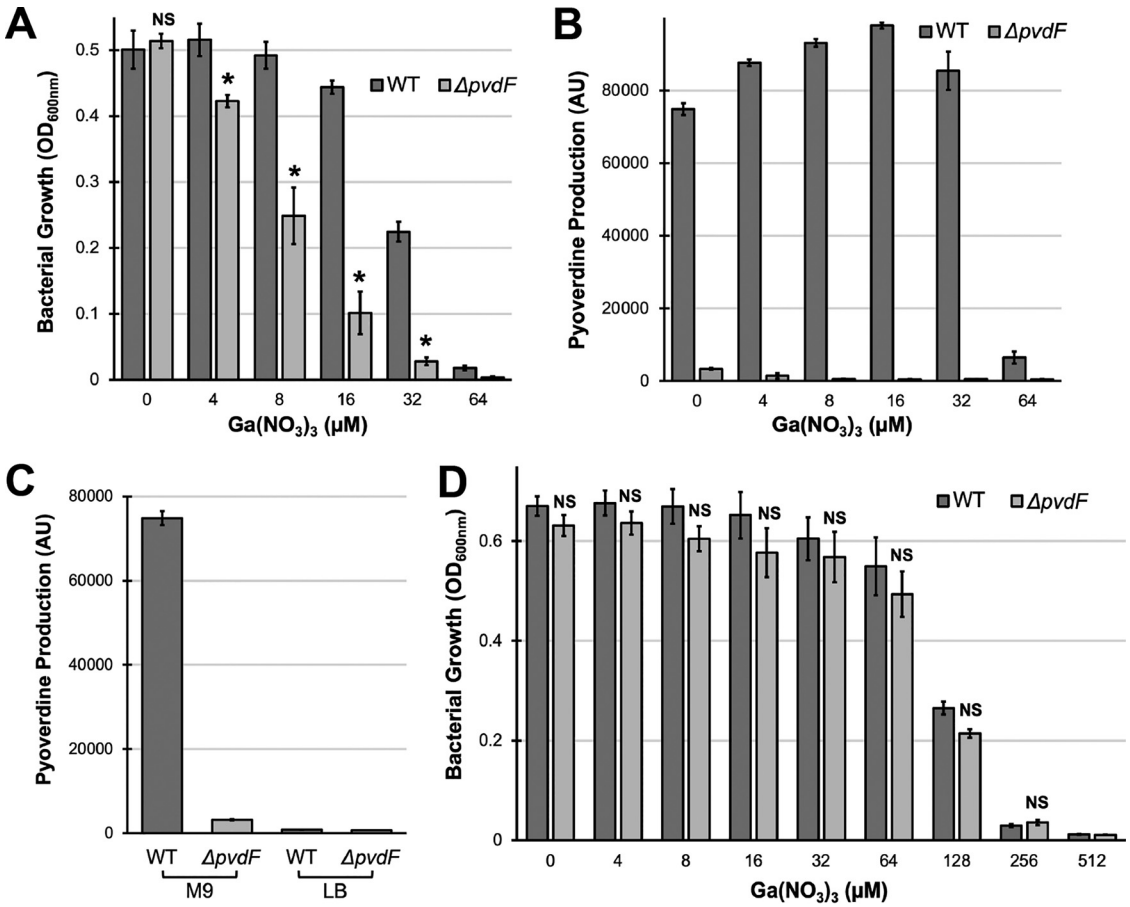

FIG 1 Pyoverdine production decreases *P. aeruginosa* susceptibility to $Ga(NO_3)_3$. (A and B) Bacterial growth (A) and pyoverdine production (B) by wild-type (WT) *P. aeruginosa* PAO1 and a pyoverdine biosynthetic mutant (PAO1Δ*pvdF*) in the presence of $Ga(NO_3)_3$ measured after 12 h incubation in M9 medium. (C) Pyoverdine production (in arbitrary units [AU]) by PAO1 and PAO1Δ*pvdF* in M9 and LB media. (D) Bacterial growth by PAO1 and PAO1Δ*pvdF* in the presence of $Ga(NO_3)_3$ in LB medium. Error bars represent standard errors of the mean (SEM) of three biological replicates. Statistical significance (Student's *t* test) is indicated as follows: *, $P < 0.01$; NS, not significant ($P > 0.05$).

between 5-FC and $Ga(NO_3)_3$ (Fig. 2A). Bacteria were treated with a single concentration of 5-FC (100 μM), which substantially inhibits pyoverdine production but not bacterial growth (Fig. 2B), and a gradient of $Ga(NO_3)_3$. 5-FC increased the bacteriostatic activity of gallium(III) at concentrations as low as 8 μM (Fig. 2A). To eliminate alternative explanations, we performed this same test with an isogenic Δ*pvdF* mutant. 5-FC had no effect on gallium-mediated growth inhibition in the Δ*pvdF* mutant (Fig. 2C), demonstrating that this synergistic interaction is pyoverdine dependent.

To investigate whether this *in vitro* synergy translates to the mitigation of bacterial virulence *in vivo*, we tested a range of drug combinations in a *C. elegans* pathogenesis model (14), where we previously showed that 5-FC rescues *C. elegans* in a pyoverdine-dependent manner (21). To explore the effects of gallium- and 5-FC-mediated growth inhibition in this model, we exposed worms to the pathogen for a longer period of time (~65-h incubation compared to ~42 h) to observe antivirulence (21). Under these conditions, 5-FC had minimal effect on pathogen virulence except at the highest concentration tested, 128 μM (Fig. 3A to C). It is important to note that this concentration is still physiologically relevant. We observed strong synergistic interactions between 5-FC and $Ga(NO_3)_3$ at several concentrations, where the drug combination resulted in near complete rescue of the host (Fig. 3B and C). To analyze these interactions in a broader context, we visualized the synergy scores for each drug combination using

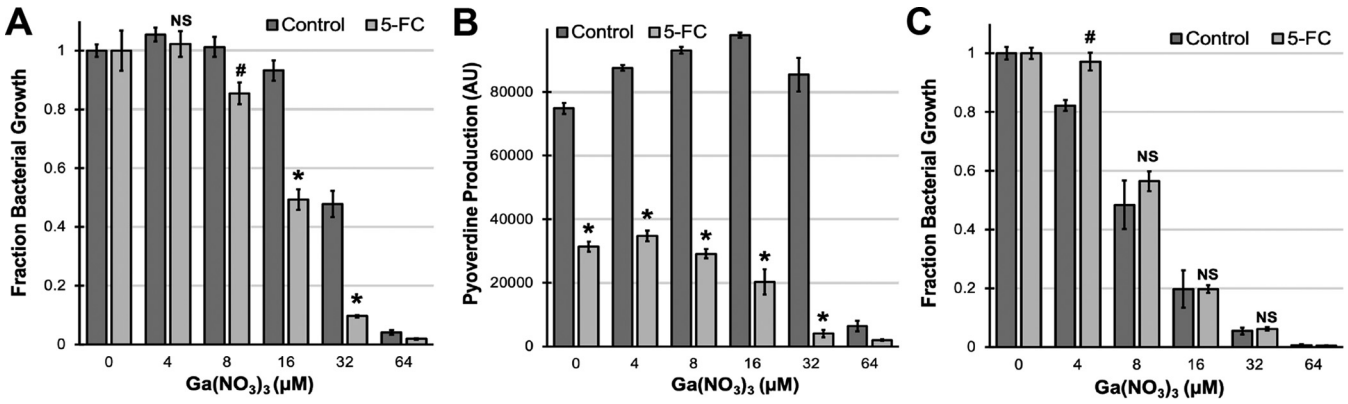

FIG 2 5-Fluorocytosine synergizes with $Ga(NO_3)_3$ to inhibit bacterial growth. (A to C) Bacterial growth (A) and pyoverdine production (B) by wild-type *P. aeruginosa* PAO1 or pyoverdine biosynthetic mutant PAO1Δ*pvdF* (C) in the presence of 100 μM 5-fluorocytosine (5-FC) and various concentrations of Ga $(NO_3)_3$ measured after 12 h incubation in M9 medium. Error bars represent SEM for four biological replicates. Statistical significance (Student's *t* test) is indicated as follows: *, $P < 0.01$; #, $P < 0.05$; NS, not significant ($P > 0.05$).

SynergyFinder (Fig. 3D) (28). For several drug synergy models, including the Bliss, highest single agency (HSA), and zero interaction potency (ZIP) models (29–31), we observed average synergy scores (δ-score) around 12, which corresponds to 12% greater effect than the expected outcome based on the performance of the individual drugs (Fig. 3E) (28). In the 3 × 3 concentration window where we observe the greatest synergy (most synergistic area), the combination of 5-FC and $Ga(NO_3)_3$ had an ~22% greater effect on pathogen virulence than expected (Fig. 3E and Fig. S2), suggesting that this is a promising drug combination to attenuate *P. aeruginosa* pathogenesis.

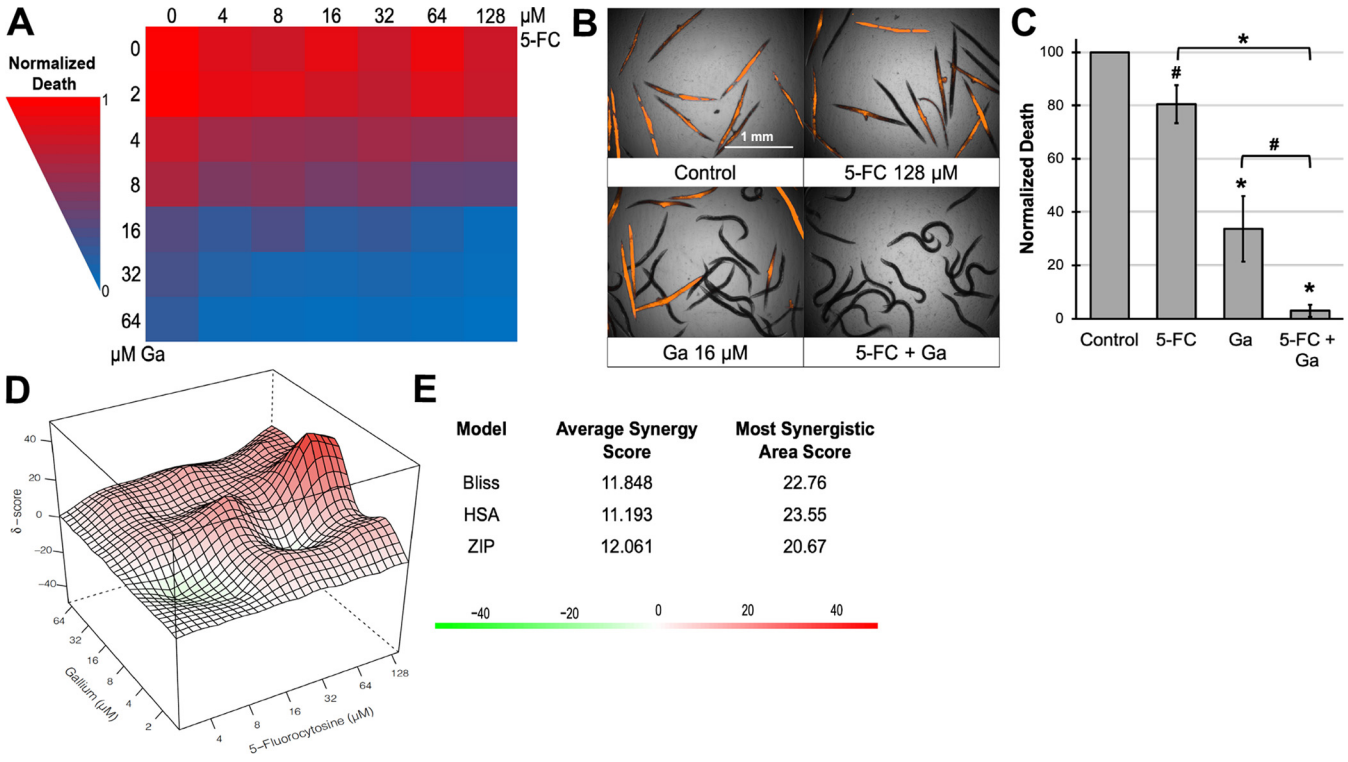

FIG 3 5-FC synergizes with $Ga(NO_3)_3$ to mitigate *P. aeruginosa* virulence. (A) Heatmap of normalized *C. elegans* death after exposure to *P. aeruginosa* in the presence of 5-fluorocytosine (5-FC) and $Ga(NO_3)_3$. Fraction host death was normalized to that of the no-drug control. (B) Fluorescent images of *C. elegans* stained with Sytox Orange cell impermeant nucleic acid stain. (C) Quantification of normalized *C. elegans* death. (D) 3-Dimensional synergy map for 5-FC and $Ga(NO_3)_3$ showing synergy scores (δ-score) for each drug combination. δ-scores were calculated based on the Bliss synergy model. (E) Average synergy scores and most synergistic area scores were calculated based on three different models. Error bars represent SEM for six biological replicates. Statistical significance (Student's *t* test) is indicated as follows: *, $P < 0.01$; #, $P < 0.05$.

Pressure to develop resistance to 5-fluorocytosine remains low despite the presence of gallium nitrate. One of the biggest motivations for the development of antivirulence therapeutics is their low selective pressure for resistance compared to conventional antimicrobials. Recently, Imperi and colleagues demonstrated that, while *P. aeruginosa* can become resistant to 5-FC through mutations in the uracil phosphoribosyltransferase (Upp) gene (32), the rate of resistance for 5-FC is orders of magnitude lower than for the analogous antibacterial compound 5-fluorouracil (33). Even after long-term exposure, 5-FC-resistant cells represented less than 0.1% of the population, which was insufficient to reduce the efficacy of pyoverdine inhibition (33).

We were interested in whether 5-FC's indirect effect on bacterial growth in the presence of gallium would increase selective pressure for developing resistance. To adapt *P. aeruginosa* in the presence of the two drugs, we grew wild-type strain PAO1 on M9 agar plates containing 250 μM 5-FC and 150 μM $Ga(NO_3)_3$. For the first 36 h, we saw no discernible bacterial growth (Fig. 4A). After this time, we noticed the appearance of spontaneously resistant colonies (Fig. 4B). Consistent with the synergistic interactions observed in liquid media, M9 agar containing either one of these two drugs supported the formation of dense bacterial lawns (Fig. 4A). However, higher concentrations of $Ga(NO_3)_3$ ($\geq$300 μM) were able to suppress bacterial growth (Fig. 4A). The presence of 300 μM gallium triggered the spontaneous emergence of resistant cells (Fig. 4B). At the same time, the combination of $Ga(NO_3)_3$ and 5-FC, even at a lower concentration of gallium, resulted in approximately half as many resistant colonies (Fig. 4C). The rate of colony growth was substantially lower on the Ga/5-FC plate (Fig. 4B), likely due to the pathogen's inability to produce pyoverdine to alleviate gallium toxicity. From this plate, we isolated 40 individual colonies and passaged them through drug-free, nutrient-rich medium for further characterization.

Bacteria from all 40 colonies grew better in the presence of gallium than the parental strain (Fig. 4D and Fig. S3A), indicating that mutants have bona fide resistance and are not merely persisters. Interestingly, all mutants remained sensitive to 5-FC (Fig. 4E and Fig. S3B). On the other hand, spontaneously resistant colonies isolated from *P. aeruginosa* grown in the presence of 5-fluorouracil (5-FU) were resistant to 5-FC-mediated pyoverdine inhibition (Fig. 4E), which is consistent with our observations that 5-FC is likely to be metabolized through 5-FU to have its effect (18, 21). These results suggest that the effect of 5-FC is through its role as an antivirulent, even in the presence of gallium. This makes it more likely that treatment will continue to exert low selective pressure for evolving resistance.

Mechanism of gallium nitrate resistance. To elucidate the mechanism of gallium resistance in the Ga/5-FC-adapted mutants, we first investigated whether increased pyoverdine production decreased sensitivity to gallium. Interestingly, none of the 40 mutants exhibited increased pyoverdine production (Fig. S3C), suggesting that the mechanism of resistance was independent of this siderophore. Previous observations by Garcia-Contreras and colleagues indicated that increased pyocyanin production could confer resistance to gallium (34), so we measured that as well. Neither the parental strain nor representative mutants produced detectable levels of pyocyanin in M9 media (data not shown).

To study pyoverdine-independent resistance to gallium(III), a *P. aeruginosa* Δ*pvdF* mutant was plated on M9 agar containing 100 μM $Ga(NO_3)_3$. Like its wild-type counterpart, we noticed the appearance of spontaneously resistant colonies (Fig. S4A), which remained resistant to gallium after passaging in drug-free medium (Fig. S4B and C). We subjected one of the mutant strains to whole-genome sequencing and discovered a single mutation, which was located in the *hitA* gene (791A→C; H264P) (Fig. 4F). *hitA* encodes a periplasmic ferric iron-binding protein belonging to the HitABC class of transporters that is responsible for the delivery of ferric iron from the periplasm to the cytoplasm (35). Mutations in *hitA* and *hitB* have previously been shown to confer resistance to $Ga(NO_3)_3$ in a transposon mutagenesis screen (34).

We sequenced the genomes of three Ga/5-FC-adapted mutants to determine whether they carried similar mutations. Each mutant exhibited monogenic mutations:

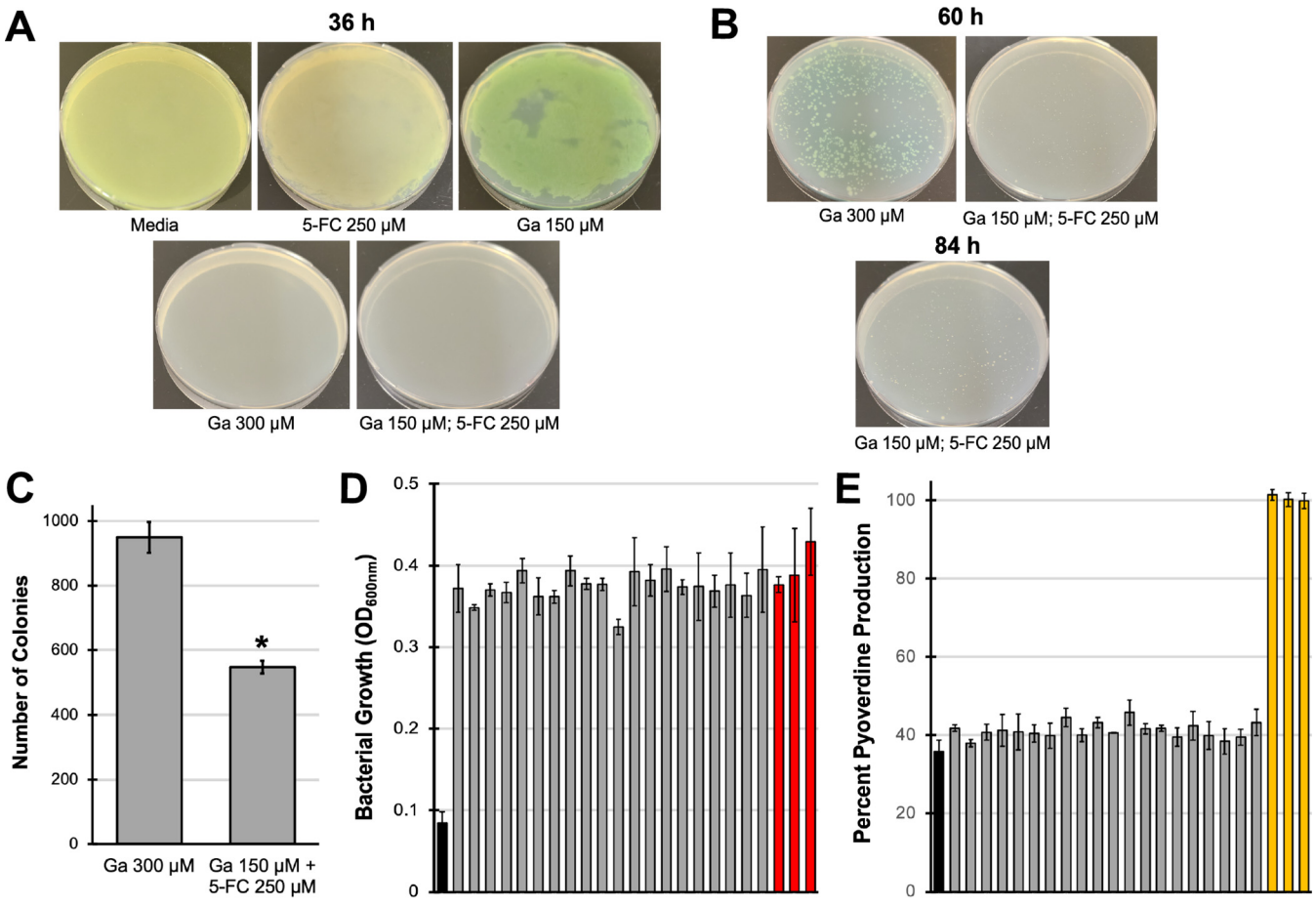

F

Mutant	Gene	Function	Mutation
ΔpvdF Ga^R	*hitA* (PA4687)	ferric iron-binding periplasmic protein	H264P
Ga/5-FC R1	PA3538	ABC transporter ATP-binding protein	E162D
Ga/5-FC R2	*hitB* (PA4688)	ferric iron ABC transporter permease	Δ3 bp (1149-1151nt) Y383*
Ga/5-FC R3	PA3538	ABC transporter ATP-binding protein	E162D
5FU R1	*upp* (PA4646)	uracil phosphoribosyltransferase	Δ42 bp (392-433nt)

FIG 4 *P. aeruginosa* mutants adapted to Ga/5-FC remain sensitive to 5-FC. (A and B) Photographs of *P. aeruginosa* PAO1 grown on M9 agar plates supplemented with 5-fluorocytosine, $Ga(NO_3)_3$, or both after 36-h (A) or 60- to 84-h (B) incubation at 37°C. (C) Number of spontaneously resistant colonies counted after 60 h on 300 μM $Ga(NO_3)_3$ or 84 h on 150 μM $Ga(NO_3)_3$ and 250 μM 5-FC. (D) Bacterial growth in M9 medium supplemented with 64 μM Ga $(NO_3)_3$ for PAO1 parental strain (black), resistant colonies from the Ga/5-FC plate (gray), and resistant colonies from the 300 μM $Ga(NO_3)_3$ plate (red). (E) Percent pyoverdine production in M9 medium supplemented with 100 μM 5-FC for the PAO1 parental strain (black), resistant colonies from the Ga/5-FC plate (gray), and resistant colonies isolated from a plate containing 1 mM 5-fluorouracil (5-FU) (yellow). Pyoverdine production was normalized to that of the no-drug control. (F) Mutations found in various $Ga(NO_3)_3$ or 5-FU-resistant mutants. Error bars in panel C represent SEM for four biological replicates. Error bars in panels D and E represent SEM for two biological replicates. *, $P < 0.01$ by Student's *t* test. nt, nucleotide.

one mutant had a nonsense mutation in *hitB*, while the other two mutants carried the same glutamic acid-to-aspartic acid substitution (E162D) in the PA3538 gene (Fig. 4F). As Guo and colleagues demonstrated that PA3538, in combination with *hitAB*, allows the transport of both iron(III) and gallium(III) into *E. coli*, which normally lacks this transport function (35), it is likely that PA3538 represents the missing HitC protein for *P. aeruginosa*. Interestingly, none of these mutants carried mutations in *upp*, while the 5-FU-adapted strain exhibited a 42-bp deletion in this gene (Fig. 4F).

Tetracyclines inhibit pyoverdine production. To test whether $Ga(NO_3)_3$ synergizes with other pyoverdine inhibitors, we turned to bacterial translational inhibitors. Pyoverdine biosynthesis requires at least 14 enzymes, including 3 large peptide synthetases, PvdL, PvdD, and PvdJ, that produce the 8- to 11-amino-acid side chain

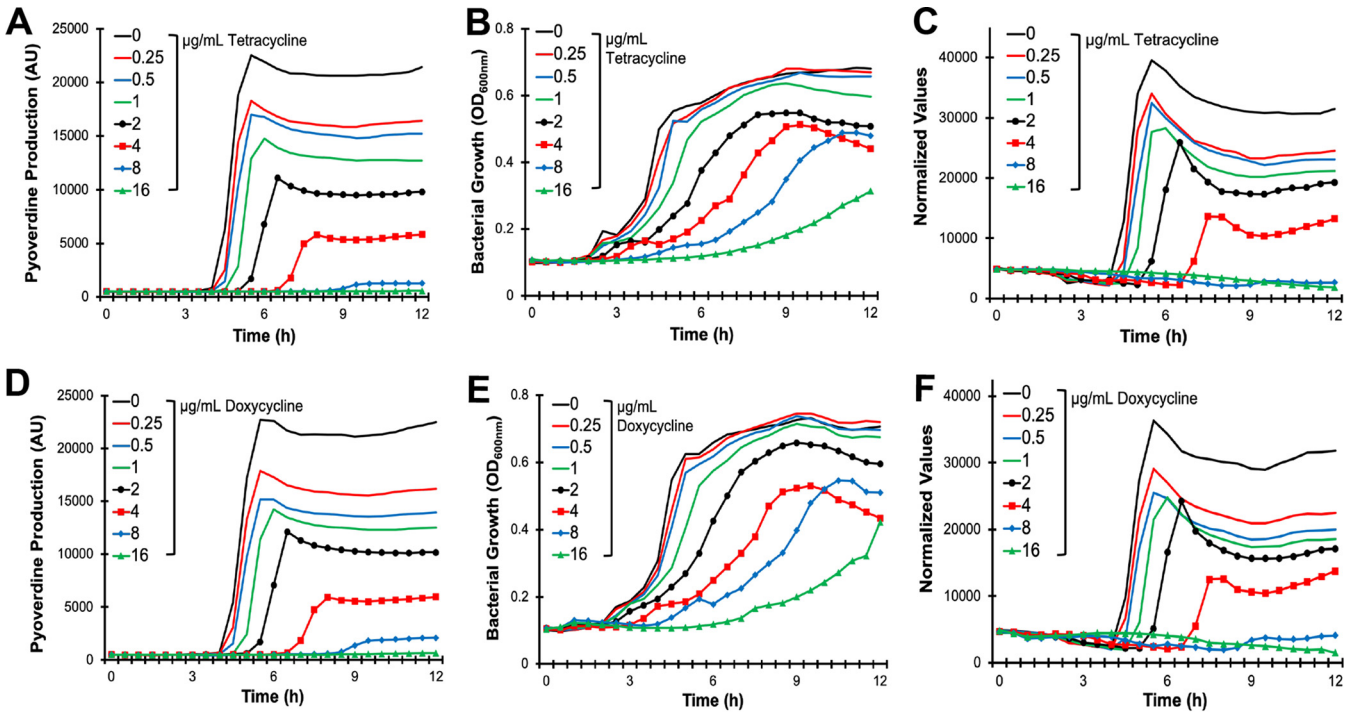

FIG 5 Tetracycline-class antibiotics inhibit pyoverdine production. (A to C) Bacterial growth (A), pyoverdine production (B), and pyoverdine production normalized to bacterial growth (C) of *P. aeruginosa* PAO1 in the presence of tetracycline. (D to F) Bacterial growth (D), pyoverdine production (E), and pyoverdine production normalized to bacterial growth (F) of *P. aeruginosa* PAO1 in the presence of doxycycline.

attached to the dihydroxyquinoline core (36). The large size of these proteins (each is greater than 2,000 amino acids) is likely to make them more sensitive to translational inhibition. We predicted that tetracycline-class antibiotics, which inhibit the 30S ribosomal subunit, would limit pyoverdine production, even at concentrations insufficient to compromise growth. We tested this by inoculating wild-type *P. aeruginosa* into media containing various concentrations of tetracycline (Fig. 5A to C) or doxycycline (Fig. 5D to F) and measured bacterial growth and pyoverdine production. We observed a decrease in pyoverdine production, even at concentrations where bacterial growth was unaffected. Higher (but still clinically relevant) concentrations of tetracycline-class antibiotics exhibited a strong bacteriostatic effect against *P. aeruginosa* and nearly abolished pyoverdine production.

We tested whether this was also true for gentamicin, an aminoglycoside antibiotic that also inhibits the 30S ribosomal subunit. As expected, gentamicin significantly curtailed pyoverdine production at subinhibitory concentrations (Fig. 6A to D). We extended this finding using *P. aeruginosa* PA2-61, a tetracycline- and gentamicin-resistant isolate from a pediatric cystic fibrosis patient (7). In this isolate, tetracycline maintained its bacteriostatic and pyoverdine-inhibitory activity, while gentamicin had no effect on bacterial growth or pyoverdine production (Fig. 6E and F). Consistent with this, we identified a multidrug resistance transposon in the genome of PA2-61 that encodes the aminoglycoside acetyltransferase AAC(6′)-IIc, which confers resistance to gentamicin, and two copies of an OXA-2 beta-lactamase (Fig. 6G). For cystic fibrosis isolates susceptible to gentamicin but resistant to tetracycline (PA2-72 and PA3-29) (7), both drugs substantially curtailed bacterial growth and pyoverdine production (Fig. S5).

One explanation for the discrepancy between the effects of tetracycline and gentamicin may arise from common mechanisms that provide resistance to these antibiotics. Tetracycline resistance in *P. aeruginosa* primarily occurs through the activity of multidrug efflux pumps (37, 38), while bacteria often biochemically modify aminoglycosides to render them inactive (39). Some *P. aeruginosa* strains carry versions of the

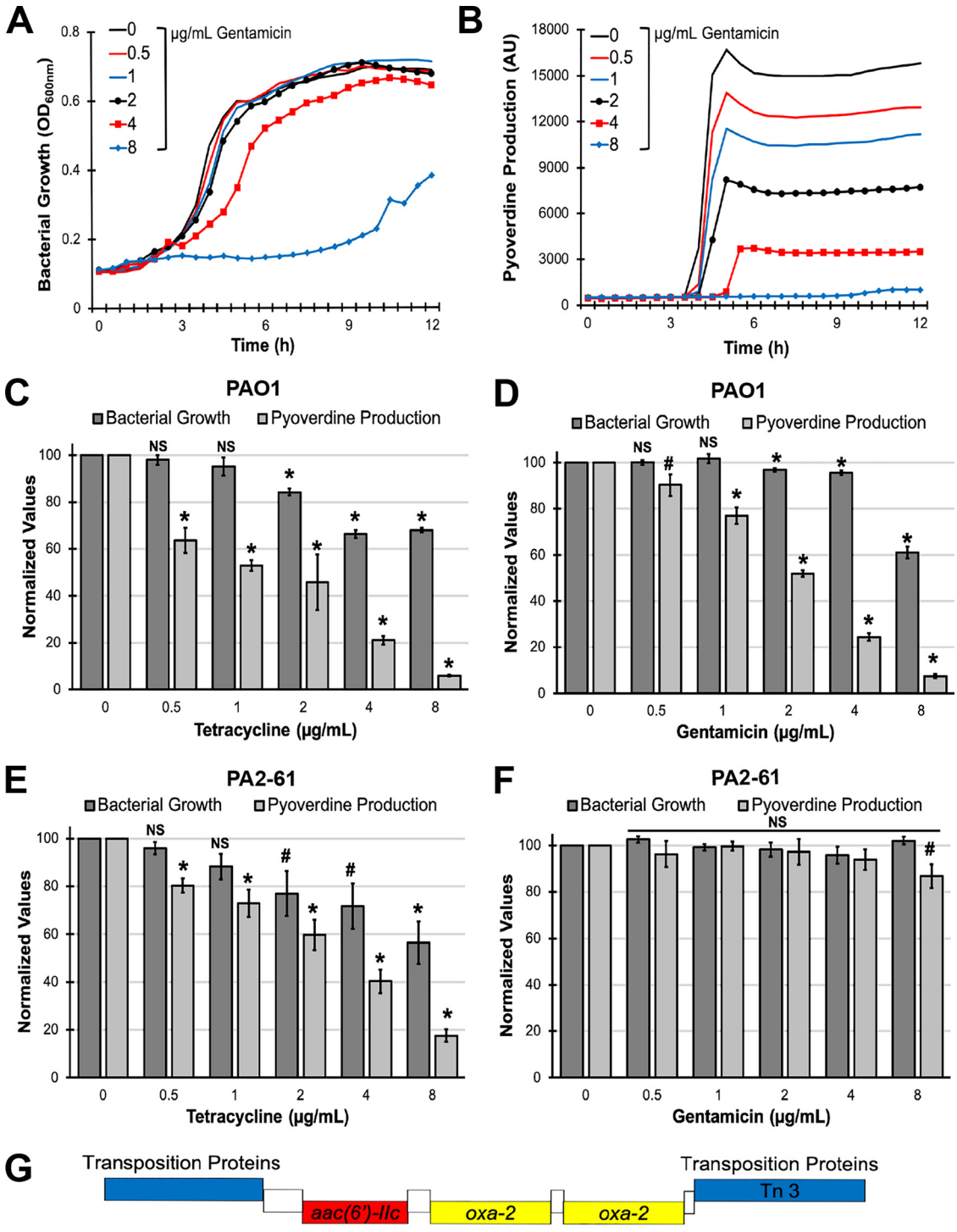

FIG 6 Gentamicin inhibits pyoverdine production only in drug-susceptible strains of *P. aeruginosa*. (A and B) Bacterial growth (A) and pyoverdine production (B) of *P. aeruginosa* PAO1 in the presence of gentamicin. (C to F) Relative bacterial growth and pyoverdine production of *P. aeruginosa* PAO1 (C and D) or cystic fibrosis isolate PA2-61 (E and F) in the presence of tetracycline or gentamicin measured after 12 h of incubation in M9 medium. Values were normalized to those of the no-drug control. (G) Diagram of the multidrug resistance transposon found in PA2-61. The *aac(6′)-Ilc* gene expresses an aminoglycoside acetyltransferase conferring resistance to gentamicin. *oxa-2* encodes a beta-lactamase. Error bars represent SEM for three biological replicates. Statistical significance (Student's *t* test) is indicated as follows: *, $P < 0.01$; #, $P < 0.05$; NS, not significant ($P > 0.05$).

tetracycline-inactivating enzyme *tet*(X) from *Bacterioides fragilis* (40, 41), which is a potential alternative explanation. We consider this less probable, however, as possession of a tetracycline-inactivating enzyme remains a rare, but currently emerging, phenotype in *P. aeruginosa* (42). Of these two mechanisms, inactivation of antibiotics is more likely to restore translational activity because it permanently reduces the concentration of the compound, rather than simply reducing intracellular concentrations. This allows tetracycline to continue to inhibit pyoverdine production. For these reasons, in subsequent experiments, our efforts focused on tetracycline as a better pyoverdine inhibitor than gentamicin.

Tetracycline synergizes with gallium nitrate to inhibit *P. aeruginosa*. Unlike 5-FC, tetracycline exhibits antimicrobial activity, so we tested a gradient of concentrations of both tetracycline and $Ga(NO_3)_3$ (Fig. 7A). The combination of 18 μM (8 μg/ml) tetracycline and 32 μM gallium was able to effectively curtail *P. aeruginosa* growth (Fig. 7A). We used SynergyFinder (28) to more accurately evaluate the interactions between tetracycline and gallium. We observed modest, concentration-specific, synergistic interactions between the two drugs in wild-type *P. aeruginosa* (δ-score $>$ 5) with the combination performing on average ~6% better than the expected outcome based on the Bliss synergy model. While this average score was below the customary cutoff for strong synergy (δ-score $>$ 10), the drug combination narrowly exceeded this standard in the area of maximal synergy (Fig. 7C). We observed similar results for the highest single agency and zero interaction potency synergy models (Fig. S6). As anticipated, no synergy was seen in the pyoverdine biosynthetic mutant, where we observed generally antagonistic interactions between the two compounds (Fig. 7B and D and Fig. S6).

It is a well-established paradigm that pyoverdine supports biofilm formation by facilitating iron acquisition (43, 44), so we also tested whether the combination of tetracycline and gallium(III) was able to effectively inhibit *P. aeruginosa* biofilm formation. As anticipated, the combination strongly compromised biofilm development (Fig. 7E and F). Finally, we tested this drug combination in a *C. elegans* pathogenesis model. While tetracycline and $Ga(NO_3)_3$ exhibited a modest attenuation of virulence on their own, the combination of the two provided essentially complete rescue (Fig. 8).

DISCUSSION

The rise of antimicrobial resistance is universally recognized as a critical threat to humanity. Despite this looming danger, antimicrobial development has waned, receiving little support from disinterested pharmaceutical programs or governments with other legislative priorities. The most effective governmental programs that have arisen involve stewardship and aim to stem further development of drug resistance by restricting the use of particular antibiotics. Unfortunately, these programs will not lead to the development of new treatments, and their efforts are stymied by regulatory apathy in other nations.

One popular alternative to the development of completely new chemical entities is to repurpose or reposition drugs that are already approved for other uses (45–47). For example, we recently reported that cancer chemotherapeutics (21) and the insulin mimetic demethylasterriquinone B1 (48) have some potential for being repurposed as antimicrobials. Since the biological characteristics are already known for compounds approved by the U.S. FDA, preliminary safety studies are much simpler, and scientists can move directly into efficacy studies.

Because gallium(III) is already FDA approved for some indications, it has been explored for repurposing as an antipseudomonal agent. This led to discoveries that gallium effectively treats *P. aeruginosa* infections in mice (22, 23). However, several obstacles limit the potential of this treatment, such as the relatively straightforward acquisition of resistance via mutation of *hitAB* (a ferric iron transporter), loss of pyochelin [which is involved in gallium(III) import], or the development of gallium efflux activity (26, 34, 49). Pyoverdine production is also known to decrease the efficacy of gallium(III) treatment (24), as we demonstrated here as well. This is likely to be a consequence of

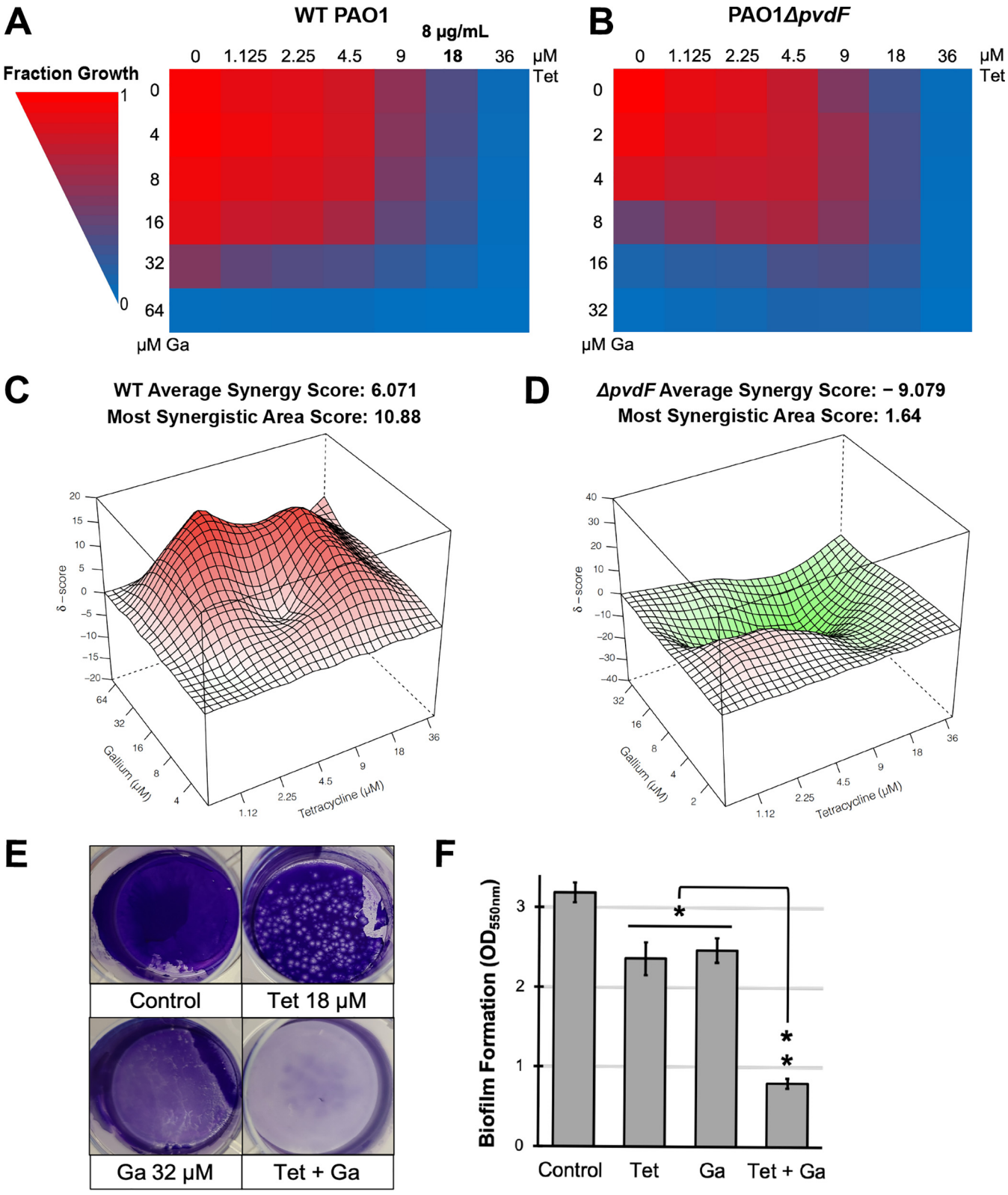

FIG 7 Tetracycline synergistically potentiates $Ga(NO_3)_3$. (A and B) Heatmap of PAO1 (A) or PAO1Δ*pvdF* (B) fraction bacterial growth in the presence of specified concentrations of tetracycline (Tet) and $Ga(NO_3)_3$ measured after 12 h of incubation in M9 medium. Values were normalized to those of the no-drug control. (C and D) 3-Dimensional synergy maps for tetracycline and $Ga(NO_3)_3$ showing synergy scores (δ-score) for each drug combination for wild-type PAO1 (C) and PAO1Δ*pvdF* (D). δ-scores were calculated based on the Bliss synergy model. (E) Photograph of *P. aeruginosa* biofilms stained with crystal violet after 20-h growth in M9 medium. (F) Quantification of crystal violet staining after acetic acid solubilization. Error bars represent SEM for three biological replicates. *, $P < 0.01$ by Student's *t* test.

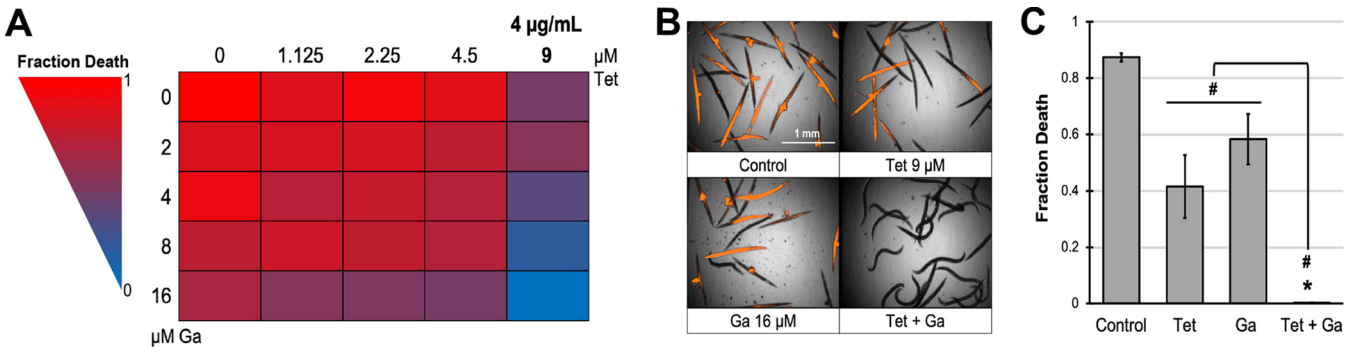

FIG 8 Tetracycline and gallium effectively mitigate *P. aeruginosa* virulence against *C. elegans*. (A) Heatmap of fraction *C. elegans* death after exposure to *P. aeruginosa* in the presence of tetracycline and $Ga(NO_3)_3$. (B) Fluorescent images of *C. elegans* stained with Sytox Orange cell impermeant nucleic acid stain. (C) Quantification of fraction *C. elegans* death. Error bars represent SEM for three biological replicates. Statistical significance (Student's *t* test) is indicated as follows: *, $P < 0.01$; #, $P < 0.05$.

irreversible sequestration of the metal by pyoverdine. While both pyoverdine-gallium and ferripyoverdine translocate into the bacterium, pyoverdine-gallium accumulates in the periplasm (27). In the periplasm, iron(III) is reduced, lowering pyoverdine's affinity and allowing the ferrous iron to be transported into the cytoplasm and the pyoverdine to be exported for reuse. Since gallium is redox inactive, the affinity is unchanged, and the metal cannot be released. Pyoverdine-gallium is also less efficiently translocated into the cell than ferripyoverdine (50) though similar observations were also made for pyochelin-gallium (51). The difference between the two siderophores is likely due to their affinities toward ferric iron and gallium. Pyochelin exhibits lower affinity toward ferric iron and is presumed to release the metal in its oxidized state, allowing pyochelin to function as a gallium shuttle rather than as a sink. On the basis of these principles, Frangipani and colleagues have demonstrated that the pyochelin-gallium complex is actually a more effective growth inhibitor than gallium nitrate alone (26). Similar observations have been previously made for the pyochelin-vanadium complex (52).

Another potential method to improve gallium(III) effect is to combine it with a conventional antimicrobial. This approach has also been documented, as Goss and colleagues investigated the interactions between gallium nitrate and a panel of antipseudomonal antibiotics. Gallium synergized with colistin and piperacillin-tazobactam but had no effect on the inhibitory effects of ceftazidime, ciprofloxacin, or aztreonam (22). Most notable, however, was that gallium exhibited antagonism with tobramycin, partially restoring bacterial growth inhibited by the antibiotic (22). This finding challenges the potential of gallium(III) as an antipseudomonal agent since tobramycin is currently the standard of care drug for inhaled antibiotic therapy in cystic fibrosis patients (53). Thus, the identification of additional therapeutics that exhibit either synergistic or additive interactions with gallium would be crucial for its clinical applicability. For instance, Halwani and colleagues demonstrated that the liposomal delivery of gallium and gentamicin is substantially more effective in inhibiting *P. aeruginosa* than the free drug treatment, even in a highly resistant clinical isolate (54).

In this report, we have demonstrated that pyoverdine inhibitors may be useful in combination with gallium(III). 5-Fluorocytosine (5-FC) and tetracycline synergized with gallium(III) to inhibit bacterial growth *in vitro* and mitigate *P. aeruginosa* virulence *in vivo*. Antivirulents such as 5-FC are considered a promising new class of therapeutics due to their presumably low selective pressure for resistance compared to conventional antimicrobials (55). However, this advantage remains controversial since infection conditions can provide selective pressure for pathogens to develop resistance against these drugs and become more pathogenic. This is likely the case for 5-FC because the molecule reduces pyoverdine production, interfering with iron uptake. *P. aeruginosa* can also easily acquire resistance through mutations in *upp*, its uracil phosphoribosyltransferase (32). However, we observed low pressure for resistance to 5-FC in the presence of gallium, even when 5-FC indirectly contributes to growth inhibition,

suggesting that therapeutics that do not directly and overtly exhibit antibacterial activity may indeed have a longer shelf life than antibiotics.

However, it is also important to note that the synergy between gallium(III) and 5-FC or tetracycline depends on effectively limiting pyoverdine production. Unfortunately, *P. aeruginosa* clinical isolates constitute a highly diverse set of strains with often heterogeneous phenotypes. For instance, we recently reported that approximately one-third of *P. aeruginosa* cystic fibrosis isolates we tested from pediatric cystic fibrosis patients lost the ability to produce pyoverdine (7). Martin and colleagues have made similar observations from cystic fibrosis patient sputum samples (56). Others have taken this a step farther and demonstrated that *P. aeruginosa* adapts its iron acquisition strategy within the cystic fibrosis lung by transitioning from pyoverdine-mediated ferric iron uptake toward heme assimilation/utilization (57, 58).

Nevertheless, pyoverdine remains a critical acute virulence factor in a majority of *P. aeruginosa* clinical isolates. Pyoverdine production can also be rapidly measured from bacterial cultures or directly detected from patient samples using spectrophotometric tools due to its distinct spectral properties (56), allowing personalized pyoverdine-based treatments to be used. Identifying additional pyoverdine inhibitors (e.g., fluoropyrimidines, twin arginine translocase inhibitors [59, 60], quorum-sensing inhibitors [61–63], etc.) and investigating their interactions with gallium may help optimize gallium nitrate as an antipseudomonal therapeutic.

MATERIALS AND METHODS

Bacterial strains and growth conditions. *P. aeruginosa* strain PAO1, pyoverdine biosynthetic mutant (PAO1Δ*pvdF*), and pyochelin biosynthetic mutant (PAO1Δ*pchBA*) were provided by Dieter Haas. Deidentified *P. aeruginosa* isolates from pediatric cystic fibrosis patients were provided by Carolyn Cannon (7). For all experiments, *P. aeruginosa* was grown in modified M9 medium (1% 5× M9 salts [Difco], 3% low-iron Casamino Acids [Difco], 1 mM $MgSO_4$, 1 mM $CaCl_2$) after initial inoculation of 100-fold diluted overnight culture. Bacteria were grown in 96-well plates for 12 h at 37°C. Bacterial growth (absorbance at 600 nm) and pyoverdine production (excitation [Ex.], 405 nm; emission [Em.], 406 nm) were measured using a Cytation5 multimode plate reader (BioTek).

***P. aeruginosa* whole-genome sequence analysis.** Bacterial genomic DNA was purified from overnight culture using DNeasy UltraClean Microbial kit (Qiagen). Paired-end Illumina sequencing was performed by the Microbial Genome Sequencing Center (MiGS) (Pittsburgh, PA) for at least 40× genome coverage. For the identification of aminoglycoside-modifying enzymes, raw sequences were first assembled via SPAdes (64) and annotated via Prokka (65). Mutation analysis in gallium-resistant mutants was performed using *breseq* (66).

***P. aeruginosa* biofilm formation assay.** *P. aeruginosa* bacteria were grown in M9 medium after initial inoculation of 100-fold diluted overnight culture in 12-well plates (1 ml per well) at 30°C for 20 h. *P. aeruginosa* biofilms were stained with 1 ml crystal violet solution (0.1% crystal violet in 20% ethanol) for 30 min after aspirating the culture supernatant. After the biofilms were gently washed in S basal buffer twice, the stained biofilms were dried at 37°C. To quantify biofilm formation, the crystal violet stain was solubilized in 30% acetic acid, and absorbance at 550 nm was measured using a Cytation5 multimode plate reader (BioTek) (67).

***C. elegans* pathogenesis assay.** *C. elegans-P. aeruginosa* liquid killing was performed as previously described (68). In brief, *C. elegans* nematodes were treated with *P. aeruginosa* in liquid kill medium (25% SK medium [0.3% NaCl, 0.35% Bacto peptone in water] in S basal buffer [100 mM NaCl, 50 mM potassium phosphate {pH 6.0}]) after initial inoculation of saturated overnight culture to an optical density at 600 nm (OD_{600}) of 0.03 in 384-well plates. After 68 h of incubation at 25°C, all wells were extensively washed with S basal buffer and treated with Sytox Orange nucleic acid stain for 12 h (ThermoFisher Scientific) to label dead organisms. Bright-field and fluorescent images were acquired on a Cytation5 multimode plate reader (BioTek) and analyzed via Cell Profiler (www.cellprofiler.org) using a previously established pipeline (69).

Drug interaction analysis. Drug interactions and synergy scores (δ-scores) were calculated using SynergyFinder 2.0, an online tool based on the Bliss, highest single agency (HSA), and zero interaction potency (ZIP) synergy models (28).

SUPPLEMENTAL MATERIAL

Supplemental material is available online only.

FIG S1, TIF file, 1.8 MB.

FIG S2, TIF file, 2.3 MB.

FIG S3, TIF file, 1.8 MB.

FIG S4, TIF file, 2.2 MB.

FIG S5, TIF file, 0.9 MB.
FIG S6, TIF file, 1.4 MB.

ACKNOWLEDGMENTS

This work has been supported by grants from the National Institutes of Health (NIGMS R35GM129294 to N.V.K.), and the Cystic Fibrosis Foundation (KIRIEN20I0 to N.V.K. and KANG19H0 and KANG21H0 to D.K.). The funders had no role in study design, data collection and analysis, decision to publish, or preparation of the manuscript.

REFERENCES

1. Kollef MH, Chastre J, Fagon JY, Francois B, Niederman MS, Rello J, Torres A, Vincent JL, Wunderink RG, Go KW, Rehm C. 2014. Global prospective epidemiologic and surveillance study of ventilator-associated pneumonia due to Pseudomonas aeruginosa. Crit Care Med 42:2178–2187. https://doi.org/10.1097/CCM.0000000000000510.
2. Tumbarello M, De Pascale G, Trecarichi EM, Spanu T, Antonicelli F, Maviglia R, Pennisi MA, Bello G, Antonelli M. 2013. Clinical outcomes of Pseudomonas aeruginosa pneumonia in intensive care unit patients. Intensive Care Med 39:682–692. https://doi.org/10.1007/s00134-013-2828-9.
3. Lansbury L, Lim B, Baskaran V, Lim WS. 2020. Co-infections in people with COVID-19: a systematic review and meta-analysis. J Infect 81:266−275. https://doi.org/10.1016/j.jinf.2020.05.046.
4. Langford BJ, So M, Raybardhan S, Leung V, Westwood D, MacFadden DR, Soucy JR, Daneman N. 2020. Bacterial co-infection and secondary infection in patients with COVID-19: a living rapid review and meta-analysis. Clin Microbiol Infect 26:1622−1629. https://doi.org/10.1016/j.cmi.2020.07.016.
5. Lanoix JP, Pluquet E, Lescure FX, Bentayeb H, Lecuyer E, Boutemy M, Dumont P, Jounieaux V, Schmit JL, Dayen C, Douadi Y. 2011. Bacterial infection profiles in lung cancer patients with febrile neutropenia. BMC Infect Dis 11:183. https://doi.org/10.1186/1471-2334-11-183.
6. Lyczak JB, Cannon CL, Pier GB. 2002. Lung infections associated with cystic fibrosis. Clin Microbiol Rev 15:194–222. https://doi.org/10.1128/CMR.15.2.194-222.2002.
7. Kang D, Revtovich AV, Chen Q, Shah KN, Cannon CL, Kirienko NV. 2019. Pyoverdine-dependent virulence of Pseudomonas aeruginosa isolates from cystic fibrosis patients. Front Microbiol 10:2048. https://doi.org/10.3389/fmicb.2019.02048.
8. Skaar EP. 2010. The battle for iron between bacterial pathogens and their vertebrate hosts. PLoS Pathog 6:e1000949. https://doi.org/10.1371/journal.ppat.1000949.
9. Takase H, Nitanai H, Hoshino K, Otani T. 2000. Impact of siderophore production on Pseudomonas aeruginosa infections in immunosuppressed mice. Infect Immun 68:1834–1839. https://doi.org/10.1128/IAI.68.4.1834-1839.2000.
10. Ankenbauer R, Sriyosachati S, Cox CD. 1985. Effects of siderophores on the growth of Pseudomonas aeruginosa in human serum and transferrin. Infect Immun 49:132–140. https://doi.org/10.1128/iai.49.1.132-140.1985.
11. Meyer JM, Neely A, Stintzi A, Georges C, Holder IA. 1996. Pyoverdin is essential for virulence of Pseudomonas aeruginosa. Infect Immun 64:518–523. https://doi.org/10.1128/iai.64.2.518-523.1996.
12. Lamont IL, Beare PA, Ochsner U, Vasil AI, Vasil ML. 2002. Siderophore-mediated signaling regulates virulence factor production in Pseudomonas aeruginosa. Proc Natl Acad Sci U S A 99:7072–7077. https://doi.org/10.1073/pnas.092016999.
13. Kang D, Kirienko DR, Webster P, Fisher AL, Kirienko NV. 2018. Pyoverdine, a siderophore from Pseudomonas aeruginosa, translocates into C. elegans, removes iron, and activates a distinct host response. Virulence 9:804–817. https://doi.org/10.1080/21505594.2018.1449508.
14. Kirienko NV, Kirienko DR, Larkins-Ford J, Wahlby C, Ruvkun G, Ausubel FM. 2013. Pseudomonas aeruginosa disrupts Caenorhabditis elegans iron homeostasis, causing a hypoxic response and death. Cell Host Microbe 13:406–416. https://doi.org/10.1016/j.chom.2013.03.003.
15. Kirienko NV, Ausubel FM, Ruvkun G. 2015. Mitophagy confers resistance to siderophore-mediated killing by Pseudomonas aeruginosa. Proc Natl Acad Sci U S A 112:1821–1826. https://doi.org/10.1073/pnas.1424954112.
16. Kang D, Kirienko NV. 2020. An in vitro cell culture model for pyoverdine-mediated virulence. Pathogens 10:9. https://doi.org/10.3390/pathogens10010009.
17. Minandri F, Imperi F, Frangipani E, Bonchi C, Visaggio D, Facchini M, Pasquali P, Bragonzi A, Visca P. 2016. Role of iron uptake systems in Pseudomonas aeruginosa virulence and airway infection. Infect Immun 84:2324–2335. https://doi.org/10.1128/IAI.00098-16.
18. Imperi F, Massai F, Facchini M, Frangipani E, Visaggio D, Leoni L, Bragonzi A, Visca P. 2013. Repurposing the antimycotic drug flucytosine for suppression of Pseudomonas aeruginosa pathogenicity. Proc Natl Acad Sci U S A 110:7458–7463. https://doi.org/10.1073/pnas.1222706110.
19. Kirienko DR, Kang D, Kirienko NV. 2018. Novel pyoverdine inhibitors mitigate *Pseudomonas aeruginosa* pathogenesis. Front Microbiol 9:3317. https://doi.org/10.3389/fmicb.2018.03317.
20. Wang X, Kleerekoper Q, Revtovich AV, Kang D, Kirienko NV. 2020. Identification and validation of a novel anti-virulent that binds to pyoverdine and inhibits its function. Virulence 11:1293–1309. https://doi.org/10.1080/21505594.2020.1819144.
21. Kirienko DR, Revtovich AV, Kirienko NV. 2016. A high-content, phenotypic screen identifies fluorouridine as an inhibitor of pyoverdine biosynthesis and Pseudomonas aeruginosa virulence. mSphere 1:e00217-16. https://doi.org/10.1128/mSphere.00217-16.
22. Goss CH, Kaneko Y, Khuu L, Anderson GD, Ravishankar S, Aitken ML, Lechtzin N, Zhou G, Czyz DM, McLean K, Olakanmi O, Shuman HA, Teresi M, Wilhelm E, Caldwell E, Salipante SJ, Hornick DB, Siehnel RJ, Becker L, Britigan BE, Singh PK. 2018. Gallium disrupts bacterial iron metabolism and has therapeutic effects in mice and humans with lung infections. Sci Transl Med 10:eaat7520. https://doi.org/10.1126/scitranslmed.aat7520.
23. DeLeon K, Balldin F, Watters C, Hamood A, Griswold J, Sreedharan S, Rumbaugh KP. 2009. Gallium maltolate treatment eradicates Pseudomonas aeruginosa infection in thermally injured mice. Antimicrob Agents Chemother 53:1331–1337. https://doi.org/10.1128/AAC.01330-08.
24. Kaneko Y, Thoendel M, Olakanmi O, Britigan BE, Singh PK. 2007. The transition metal gallium disrupts Pseudomonas aeruginosa iron metabolism and has antimicrobial and antibiofilm activity. J Clin Invest 117:877–888. https://doi.org/10.1172/JCI30783.
25. Wang Y, Han B, Xie Y, Wang H, Wang R, Xia W, Li H, Sun H. 2019. Combination of gallium(III) with acetate for combating antibiotic resistant Pseudomonas aeruginosa. Chem Sci 10:6099–6106. https://doi.org/10.1039/c9sc01480b.
26. Frangipani E, Bonchi C, Minandri F, Imperi F, Visca P. 2014. Pyochelin potentiates the inhibitory activity of gallium on Pseudomonas aeruginosa. Antimicrob Agents Chemother 58:5572–5575. https://doi.org/10.1128/AAC.03154-14.
27. Greenwald J, Hoegy F, Nader M, Journet L, Mislin GL, Graumann PL, Schalk IJ. 2007. Real time fluorescent resonance energy transfer visualization of ferric pyoverdine uptake in Pseudomonas aeruginosa. A role for ferrous iron. J Biol Chem 282:2987–2995. https://doi.org/10.1074/jbc.M609238200.
28. Ianevski A, Giri AK, Aittokallio T. 2020. SynergyFinder 2.0: visual analytics of multi-drug combination synergies. Nucleic Acids Res 48:W488–W493. https://doi.org/10.1093/nar/gkaa216.
29. Yadav B, Wennerberg K, Aittokallio T, Tang J. 2015. Searching for drug synergy in complex dose-response landscapes using an interaction potency model. Comput Struct Biotechnol J 13:504–513. https://doi.org/10.1016/j.csbj.2015.09.001.
30. Berenbaum MC. 1989. What is synergy? Pharmacol Rev 41:93–141.
31. Bliss CI. 1939. The toxicity of poisons applied jointly. Ann Appl Biol 26:585–615. https://doi.org/10.1111/j.1744-7348.1939.tb06990.x.
32. Rezzoagli C, Wilson D, Weigert M, Wyder S, Kümmerli R. 2018. Probing the evolutionary robustness of two repurposed drugs targeting iron uptake in Pseudomonas aeruginosa. Evol Med Public Health 2018:246–259. https://doi.org/10.1093/emph/eoy026.
33. Imperi F, Fiscarelli EV, Visaggio D, Leoni L, Visca P. 2019. Activity and impact on resistance development of two antivirulence fluoropyrimidine

drugs in Pseudomonas aeruginosa. Front Cell Infect Microbiol 9:49. https://doi.org/10.3389/fcimb.2019.00049.
34. García-Contreras R, Lira-Silva E, Jasso-Chávez R, Hernández-González IL, Maeda T, Hashimoto T, Boogerd FC, Sheng L, Wood TK, Moreno-Sánchez R. 2013. Isolation and characterization of gallium resistant Pseudomonas aeruginosa mutants. Int J Med Microbiol 303:574–582. https://doi.org/10.1016/j.ijmm.2013.07.009.
35. Guo Y, Li W, Li H, Xia W. 2019. Identification and characterization of a metalloprotein involved in gallium internalization in Pseudomonas aeruginosa. ACS Infect Dis 5:1693–1697. https://doi.org/10.1021/acsinfecdis.9b00271.
36. Visca P, Imperi F, Lamont IL. 2007. Pyoverdine siderophores: from biogenesis to biosignificance. Trends Microbiol 15:22–30. https://doi.org/10.1016/j.tim.2006.11.004.
37. Dean CR, Visalli MA, Projan SJ, Sum PE, Bradford PA. 2003. Efflux-mediated resistance to tigecycline (GAR-936) in Pseudomonas aeruginosa PAO1. Antimicrob Agents Chemother 47:972–978. https://doi.org/10.1128/AAC.47.3.972-978.2003.
38. Morita Y, Tomida J, Kawamura Y. 2014. Responses of Pseudomonas aeruginosa to antimicrobials. Front Microbiol 4:422. https://doi.org/10.3389/fmicb.2013.00422.
39. Poole K. 2005. Aminoglycoside resistance in Pseudomonas aeruginosa. Antimicrob Agents Chemother 49:479–487. https://doi.org/10.1128/AAC.49.2.479-487.2005.
40. Gasparrini AJ, Markley JL, Kumar H, Wang B, Fang L, Irum S, Symister CT, Wallace M, Burnham CD, Andleeb S, Tolia NH, Wencewicz TA, Dantas G. 2020. Tetracycline-inactivating enzymes from environmental, human commensal, and pathogenic bacteria cause broad-spectrum tetracycline resistance. Commun Biol 3:241. https://doi.org/10.1038/s42003-020-0966-5.
41. Leski TA, Bangura U, Jimmy DH, Ansumana R, Lizewski SE, Stenger DA, Taitt CR, Vora GJ. 2013. Multidrug-resistant tet(X)-containing hospital isolates in Sierra Leone. Int J Antimicrob Agents 42:83–86. https://doi.org/10.1016/j.ijantimicag.2013.04.014.
42. He T, Wang R, Liu D, Walsh TR, Zhang R, Lv Y, Ke Y, Ji Q, Wei R, Liu Z, Shen Y, Wang G, Sun L, Lei L, Lv Z, Li Y, Pang M, Wang L, Sun Q, Fu Y, Song H, Hao Y, Shen Z, Wang S, Chen G, Wu C, Shen J, Wang Y. 2019. Emergence of plasmid-mediated high-level tigecycline resistance genes in animals and humans. Nat Microbiol 4:1450–1456. https://doi.org/10.1038/s41564-019-0445-2.
43. Kang D, Kirienko NV. 2018. Interdependence between iron acquisition and biofilm formation in Pseudomonas aeruginosa. J Microbiol 56:449–457. https://doi.org/10.1007/s12275-018-8114-3.
44. Banin E, Vasil ML, Greenberg EP. 2005. Iron and Pseudomonas aeruginosa biofilm formation. Proc Natl Acad Sci U S A 102:11076–11081. https://doi.org/10.1073/pnas.0504266102.
45. Pacios O, Blasco L, Bleriot I, Fernandez-Garcia L, Gonzalez Bardanca M, Ambroa A, Lopez M, Bou G, Tomas M. 2020. Strategies to combat multidrug-resistant and persistent infectious diseases. Antibiotics (Basel) 9:65. https://doi.org/10.3390/antibiotics9020065.
46. Miro-Canturri A, Ayerbe-Algaba R, Smani Y. 2019. Drug repurposing for the treatment of bacterial and fungal infections. Front Microbiol 10:41. https://doi.org/10.3389/fmicb.2019.00041.
47. Farha MA, Brown ED. 2019. Drug repurposing for antimicrobial discovery. Nat Microbiol 4:565–577. https://doi.org/10.1038/s41564-019-0357-1.
48. Hummell NA, Kirienko NV. 2020. Repurposing bioactive compounds for treating multidrug-resistant pathogens. J Med Microbiol 69:881–894. https://doi.org/10.1099/jmm.0.001172.
49. Tovar-Garcia A, Angarita-Zapata V, Cazares A, Jasso-Chavez R, Belmont-Diaz J, Sanchez-Torres V, Lopez-Jacome LE, Coria-Jimenez R, Maeda T, Garcia-Contreras R. 2020. Characterization of gallium resistance induced in a Pseudomonas aeruginosa cystic fibrosis isolate. Arch Microbiol 202:617–622. https://doi.org/10.1007/s00203-019-01777-y.
50. Braud A, Hoegy F, Jezequel K, Lebeau T, Schalk IJ. 2009. New insights into the metal specificity of the Pseudomonas aeruginosa pyoverdine-iron uptake pathway. Environ Microbiol 11:1079–1091. https://doi.org/10.1111/j.1462-2920.2008.01838.x.
51. Braud A, Hannauer M, Mislin GL, Schalk IJ. 2009. The Pseudomonas aeruginosa pyochelin-iron uptake pathway and its metal specificity. J Bacteriol 191:3517–3525. https://doi.org/10.1128/JB.00010-09.
52. Baysse C, De Vos D, Naudet Y, Vandermonde A, Ochsner U, Meyer JM, Budzikiewicz H, Schafer M, Fuchs R, Cornelis P. 2000. Vanadium interferes with siderophore-mediated iron uptake in Pseudomonas aeruginosa. Microbiology (Reading) 146:2425–2434. https://doi.org/10.1099/00221287-146-10-2425.
53. Mogayzel PJ, Jr, Naureckas ET, Robinson KA, Brady C, Guill M, Lahiri T, Lubsch L, Matsui J, Oermann CM, Ratjen F, Rosenfeld M, Simon RH, Hazle L, Sabadosa K, Marshall BC, Cystic Fibrosis Foundation Pulmonary Clinical Practice Guidelines Committee. 2014. Cystic Fibrosis Foundation pulmonary guideline. Pharmacologic approaches to prevention and eradication of initial Pseudomonas aeruginosa infection. Ann Am Thorac Soc 11:1640–1650. https://doi.org/10.1513/AnnalsATS.201404-166OC.
54. Halwani M, Yebio B, Suntres ZE, Alipour M, Azghani AO, Omri A. 2008. Co-encapsulation of gallium with gentamicin in liposomes enhances antimicrobial activity of gentamicin against Pseudomonas aeruginosa. J Antimicrob Chemother 62:1291–1297. https://doi.org/10.1093/jac/dkn422.
55. Kang D, Zhang L, Kirienko NV. 2021. High-throughput approaches for the identification of Pseudomonas aeruginosa antivirulents. mBio 12:02240-20. https://doi.org/10.1128/mBio.02240-20.
56. Martin LW, Reid DW, Sharples KJ, Lamont IL. 2011. Pseudomonas siderophores in the sputum of patients with cystic fibrosis. Biometals 24:1059–1067. https://doi.org/10.1007/s10534-011-9464-z.
57. Nguyen AT, O'Neill MJ, Watts AM, Robson CL, Lamont IL, Wilks A, Oglesby-Sherrouse AG. 2014. Adaptation of iron homeostasis pathways by a Pseudomonas aeruginosa pyoverdine mutant in the cystic fibrosis lung. J Bacteriol 196:2265–2276. https://doi.org/10.1128/JB.01491-14.
58. Marvig RL, Damkiær S, Khademi SMH, Markussen TM, Molin S, Jelsbak L. 2014. Within-host evolution of Pseudomonas aeruginosa reveals adaptation toward iron acquisition from hemoglobin. mBio 5:e00966-14. https://doi.org/10.1128/mBio.00966-14.
59. Massai F, Saleeb M, Doruk T, Elofsson M, Forsberg Å. 2019. Development, optimization, and validation of a high throughput screening assay for identification of Tat and type II secretion inhibitors of Pseudomonas aeruginosa. Front Cell Infect Microbiol 9:250. https://doi.org/10.3389/fcimb.2019.00250.
60. Ochsner UA, Snyder A, Vasil AI, Vasil ML. 2002. Effects of the twin-arginine translocase on secretion of virulence factors, stress response, and pathogenesis. Proc Natl Acad Sci U S A 99:8312–8317. https://doi.org/10.1073/pnas.082238299.
61. Lee JH, Kim YG, Cho MH, Kim JA, Lee J. 2012. 7-Fluoroindole as an antivirulence compound against Pseudomonas aeruginosa. FEMS Microbiol Lett 329:36–44. https://doi.org/10.1111/j.1574-6968.2012.02500.x.
62. Peppoloni S, Pericolini E, Colombari B, Pinetti D, Cermelli C, Fini F, Prati F, Caselli E, Blasi E. 2020. The beta-lactamase inhibitor boronic acid derivative SM23 as a new anti-Pseudomonas aeruginosa biofilm. Front Microbiol 11:35. https://doi.org/10.3389/fmicb.2020.00035.
63. Zhou JW, Luo HZ, Jiang H, Jian TK, Chen ZQ, Jia AQ. 2018. Hordenine: a novel quorum sensing inhibitor and antibiofilm agent against Pseudomonas aeruginosa. J Agric Food Chem 66:1620–1628. https://doi.org/10.1021/acs.jafc.7b05035.
64. Bankevich A, Nurk S, Antipov D, Gurevich AA, Dvorkin M, Kulikov AS, Lesin VM, Nikolenko SI, Pham S, Prjibelski AD, Pyshkin AV, Sirotkin AV, Vyahhi N, Tesler G, Alekseyev MA, Pevzner PA. 2012. SPAdes: a new genome assembly algorithm and its applications to single-cell sequencing. J Comput Biol 19:455–477. https://doi.org/10.1089/cmb.2012.0021.
65. Seemann T. 2014. Prokka: rapid prokaryotic genome annotation. Bioinformatics 30:2068–2069. https://doi.org/10.1093/bioinformatics/btu153.
66. Deatherage DE, Barrick JE. 2014. Identification of mutations in laboratory-evolved microbes from next-generation sequencing data using breseq. Methods Mol Biol 1151:165–188. https://doi.org/10.1007/978-1-4939-0554-6_12.
67. Kang D, Kirienko NV. 2017. High-throughput genetic screen reveals that early attachment and biofilm formation are necessary for full pyoverdine production by Pseudomonas aeruginosa. Front Microbiol 8:1707. https://doi.org/10.3389/fmicb.2017.01707.
68. Anderson QL, Revtovich AV, Kirienko NV. 2018. A high-throughput, high-content, liquid-based C. elegans pathosystem. J Vis Exp 2018:58068. https://doi.org/10.3791/58068.
69. Conery AL, Larkins-Ford J, Ausubel FM, Kirienko NV. 2014. High-throughput screening for novel anti-infectives using a C. elegans pathogenesis model. Curr Protoc Chem Biol 6:25–37. https://doi.org/10.1002/9780470559277.ch130160.